Available online at www.sciencedirect.com

SciVerse ScienceDirect

Journal of the European Ceramic Society 32 (2012) 2351–2357

www.elsevier.com/locate/jeurceramsoc

Preparation and characterization of $BaCe_{0.95}Tb_{0.05}O_{3-\alpha}$ hollow fibre membranes for hydrogen permeation

Xiaoyao Tan [a,b,*], Jian Song [b], Xiuxia Meng [b], Bo Meng [b]

[a] *Department of Chemical Engineering, Tianjin Polytechnic University, Tianjin 300387, China*
[b] *School of Chemical Engineering, Shandong University of Technology, Zibo 255049, China*

Received 13 January 2012; received in revised form 29 February 2012; accepted 1 March 2012
Available online 23 March 2012

Abstract

$BaCe_{0.95}Tb_{0.05}O_{3-\alpha}$ (BCTb) perovskite hollow fibre membranes were fabricated by spinning the slurry mixture containing 66.67 wt% BCTb powder, 6.67 wt% polyethersulphone (PESf) and 26.67 wt% N-methyl-2-pyrrolidone (NMP) followed by sintering at elevated temperatures. The influence of sintering temperature on the membrane properties was investigated in terms of crystal phase, morphology, porosity and mechanical strength. In order to obtain gas-tight hollow fibres with sufficient mechanical strength, the sintering temperature should be controlled between 1350 and 1450 °C. Hydrogen permeation through the BCTb hollow fibre membranes was carried out between 700 and 1000 °C using 50% H_2–He mixture as feed on the shell side and N_2 as sweep gas in the fibre lumen. The measured hydrogen permeation flux through the BCTb hollow fibre membranes reached up to 0.422 μmol cm^{-2} s^{-1} at 1000 °C when the flow rates of the H_2–He feed and the nitrogen sweep were 40 mL min^{-1} and 30 mL min^{-1}, respectively.

Keywords: Perovskite; Membranes; Extrusion; Sintering; Hydrogen permeation

1. Introduction

Dense mixed proton and electronic conducting ceramic membranes, mostly based on the $SrCeO_3$, $BaCeO_3$, $SrZrO_3$ and $BaZrO_3$ perovskite oxides in a general formula of ABO_3, have attracted considerable interest over the past few decades for their potential applications in hydrogen pumps (separators), fuel cells, gas sensors and catalytic membrane reactors.[1–4] Owing to many advantages such as thermal stability, chemical resistance to corrosive environments, good mechanical strength and high hydrogen permeation flux, Pd-based membranes have been extensively studied for H_2 production/separation and for dehydrogenation/hydrogenation reactions. However, the Pd-based membranes exhibit disadvantages of high Pd cost and low stability when they are in contact with CO or H_2S.[5] Compared with the hydrogen permeable Pd-based membranes, the conventional proton conducting oxide membranes being investigated generally possess much lower hydrogen permeation fluxes, i.e., ~0.02 mL (STP) cm^{-2} min^{-1} at ~900 °C under H_2/He gradients.[6] This may be partially attributed to the inherent low protonic and/or electronic conductivity of the oxide. Among the proton conducting oxides, the $BaCeO_3$-based perovskite exhibits the highest conductivity with increasing contribution of oxygen ionic conduction as temperature increases.[7] In order to improve the conducting properties of the membrane, doping with trivalent rare earth elements at the B-site is an important strategy. The doping cation plays an important role in the conductivity of the resultant perovskite oxides.[8] For example, the Tb-doped $SrCeO_3$-based perovskite possess higher protonic conductivity but significantly lower electronic conductivity because Tb cation has higher ionization potential (39.8 eV) than other trivalent cations such as Yb (25.0 eV) and Tm (23.7 eV).[9–11] On the other hand, in most previous studies the proton conducting membranes were made in the small disk form with large thicknesses (for example, 1 cm diameter and 1 mm thickness) because they are easily fabricated using conventional methods. An effective way to promote the hydrogen permeation flux is to reduce the membrane thickness, which can be achieved by using the composite

* Corresponding author at: Department of Chemical Engineering, Tianjin Polytechnic University, Tianjin 300387, China. Tel.: +86 22 83955451; fax: +86 22 83955451.
E-mail address: cestanxy@yahoo.com.cn (X. Tan).

0955-2219/$ – see front matter © 2012 Elsevier Ltd. All rights reserved.
doi:10.1016/j.jeurceramsoc.2012.03.004

membrane structure where the dense thin proton conducting ceramic film is supported on a porous substrate. For instance, when the membrane thickness was decreased to micrometer level, the hydrogen flux up to 0.1 mL (STP) cm^{-2} min^{-1} at 900 °C under H_2/He gradients was observed.[12–15] However, the composite membrane normally suffers from the problems of such as preparation complexity and difficulty of use. The multi-step preparation of the composite membranes is a time-consuming process, making them very costly. Moreover, in the membrane sintering process, the support or the dense layer tends to crack or to peel off due to the mismatch of thermal expansion between the two different materials employed. In the practical applications, cracks of the composite membrane are usually inevitable in high temperature environments unless the membranes are made from the same or similar materials.

Over the past ten years, the ceramic membranes with hollow fibre geometry have been developed via a combined phase inversion and sintering technique.[16–21] Compared to other configurations like tubular or disk-shaped membranes, the hollow fibres exhibit many advantages such as facile high-temperature sealing, thin effective membrane thickness due to the asymmetric structure, and, more importantly, larger membrane area per unit packing volume. Therefore, a high hydrogen production rate can be achieved by using a hollow fibre membrane module having large specific membrane areas, even if the permeability of the individual membrane may be low. Moreover, since the dense separation film and the porous support are made in one-step from the same ceramic material, cracks or peeling off between the two structural layers can be avoided. These appreciable advantages make the proton conducting membranes more appropriate in practical applications.

This work aims to investigate whether or not the gas tight $BaCe_{0.95}Tb_{0.05}O_{3-\alpha}$ (BCTb) perovskite hollow fibre membranes can be fabricated by the phase inversion-sintering method and to demonstrate the concept of such hollow fibre membranes for H_2 permeation. To realize this purpose, the work has involved the synthesis of qualified BCTb powder as the starting membrane material, formation of hollow fibre precursor, fibre sintering at different programs and the leaking/permeation test. A special emphasis would be placed on the influences of sintering temperature on the hollow fibre membrane properties in terms of crystalline structure, micro morphology, porosity and mechanical strength. The electrical conductivity and the hydrogen permeation performance of the resultant hollow fibre membranes have also been investigated experimentally.

2. Experimental

2.1. Fabrication of the BCTb perovskite powder and hollow fibre membranes

The $BaCe_{0.95}Tb_{0.05}O_{3-\alpha}$ (BCTb) perovskite powder was synthesized by a sol–gel method using ethylenediaminetetraacetic acid (EDTA) and citric acid (CA) as complexing agents simultaneously. $Ba(NO_3)_2$, $Ce(NO_3)_3{\cdot}6H_2O$, $Tb(NO_3)_3{\cdot}6H_2O$, all in analytical grades, were used as the raw materials for metal ion sources. The mole ratio of total metal ions to EDTA to citric acid to NH_4NO_3 in the sol was 1:1:2:10. The powder precursor obtained by the gel combustion was calcined at 1000 °C for 5 h under static air to obtain the perovskite phase. The detailed synthesis process was described elsewhere.[22] For spinning hollow fibre membrane precursors, the calcined powder was further ball-milled in the presence of alcohol for at least 10 h followed by sieving through a sifter of 200-mesh to exclude agglomerates.

The BCTb hollow fibre membranes were prepared by the phase inversion and sintering technique.[17,18] The starting suspension was composed of 66.67 wt% BCTb powder, 6.67 wt% polyethersulphone (PESf, Radel A-300, from Ameco Performance, USA) as the polymer binder and 26.67 wt% N-methyl-2-pyrrolidone (NMP, AR Grade, >99.8%, Kermel Chem Inc., Tianjin, China) as the solvent. A spinneret with the orifice diameter/inner diameter of 3.0/1.2 mm was used for spinning hollow fibre precursors. Municipal water and deionized water were used as the external and the internal coagulants, respectively. Sintering was performed at the elevated temperatures ranging from 1200 to 1500 °C with an interval of 50 °C for 5 h under ambient non-flowing air atmosphere. The heating and cooling rate applied during the whole sintering process was 2–4 °C min^{-1}.

2.2. Characterization

Microstructures of the BCTb powder and hollow cracks or peeling off fibres were observed by scanning electron microscopy (SEM) (FEI Sirion200, Netherlands). Gold sputter coating was performed on the samples under vacuum before the measurements. The crystal structures of the samples were measured by an X-ray diffractometer (XRD: D8 Advance, Germany) using Cu-Kα radiation ($\lambda = 0.15404$ nm). A continuous scan mode was used to collect 2θ data from 20° to 80° with a 0.02 sampling pitch and a 2° min^{-1} scan rate. X-ray tube voltage and current were set at 40 kV and 30 mA, respectively. The gas-tightness of the hollow fibres was measured by a gas permeation test using N_2 as the test gas.[23] The apparent density as well as the porosity of the hollow fibres was measured by the Archimedes method using DI water as medium. The density of the BCTb disk membranes with the diameter of ∅25 mm, which were prepared by statically pressing the pure BCTb powder under a pressure of 10 MPa followed by sintering at 1200–1500 °C for 5 h, was also obtained via the Archimedes method. The porosity of the hollow fibre membranes was calculated by the following equation:

$$\varepsilon = \left(1 - \frac{\rho_{hf}}{\rho_d}\right) \times 100\% \quad (1)$$

where ρ_{hf} and ρ_d are the density of the hollow fibre and the disk membranes, respectively. For each type of the hollow fibre membranes, at least three samples were taken for the measurement.

The mechanical strength of the hollow fibres was measured on a three-point bending instrument (Instron Model 5544) with a crosshead speed of 0.5 mm min^{-1}. The hollow fibre sample was

fixed on the sample holder at a distance of 26 mm. The bending strength, σ_F, was calculated from the following equation:

$$\sigma_F = \frac{8FLD}{\pi(D^4 - d^4)} \quad (2)$$

where F is the measured force at which the fracture takes place, D, d and L are the outer diameter, the inner diameter and the length (26 mm) of the hollow fibre sample, respectively. For each hollow fibre, three samples were taken for the measurement and the average bending strength value was taken as the mechanical strength of the hollow fibre membrane.

The electrical conductivity of the BCTb hollow fibre membranes was measured in hydrogen atmosphere at different temperatures with an electrochemistry workstation (Zahner IM6ex). Silver wires were attached at both ends of the sample (5 cm length) by silver paste to serve as the current and voltage electrodes. For reliable contact of the lead wires, Ag paste was applied to the sample and cured at 750 °C for 1 h in hydrogen atmosphere. Current–voltage characteristics were recorded in the current range of 0–1.0 A. All the samples showed nearly linear I–V curves. The electrical resistance was obtained from the slope of the curves by the least square method. For comparison, the conductivity of the sintered disk membrane was also measured using the four-probe D.C. method.[22]

2.3. Hydrogen permeation measurement

The hydrogen permeation flux through the hollow fibre membranes was measured using a home-made high-temperature permeation cell that was described elsewhere.[24] The hollow fibre membrane for the permeation measurement had a length of about 30 cm and was tested to be completely gas-tight at room temperature in advance. A H_2–He mixture with the molar ratio of 1:1 was fed to the shell side while nitrogen as the sweep gas was introduced in the fibre lumen to collect the permeated hydrogen. The flow rates of the H_2–He feed and the N_2 sweep gas were controlled by mass flow controllers (D08-8B/ZM, Shanxi Chuangwei Instrument Co. Ltd., China) which were calibrated with a soap bubble flow meter. The effluent flow rate of the permeate stream was also measured by the soap bubble flow meter. The composition of the permeated gas was analysed with a gas chromatograph (Agilent 6890) fitted with a carbon molecular sieve column (4 m in length) using highly pure argon as the carrier gas. The hydrogen permeation flux was calculated by:

$$J_{H_2} = \frac{V_e}{A_m}(y_{H_2} - y_{He}) \quad (3)$$

where V_e is the flow rate of the permeate stream, mol s^{-1}; y_{H_2} and y_{He} are the hydrogen the helium molar fraction in permeate stream, mol%; and A_m is the effective membrane area for hydrogen permeation, which was calculated by $A_m = (\pi(D-d)L)/(\ln(D/d))$ in which L is the effective permeation length of the hollow fibre membrane. In this study, the effective permeation length L was considered to be equivalent to the effective heating length of the furnace, i.e., 5 cm. Some helium could be detected (<0.78%) in the permeated stream indicating a small leakage occurred in the permeation cell. The amount of hydrogen detected from the leakage had to be deducted so as to obtain the net permeation fluxes. It should be noted that the membrane area beyond the central heating zone may also exhibit some hydrogen permeation, but its contribution towards the overall hydrogen flux should be much lower than the central part since the hydrogen permeability usually decreases exponentially with temperature.

3. Results and discussion

3.1. Preparation of the BCTb hollow fibre membranes

BCTb perovskite hollow fibre membranes were fabricated by the combined phase inversion and sintering method from the self-made powders. Normally the existence of larger irregular particle agglomerates is one of the unfavourable factors impeding the synthesis of highly qualified hollow fibre membranes. In order to break the large agglomerates, the calcined powders were ball-milled for 10 h followed by sieving through a sifter of 200-mesh prior to the mixing with polymeric binder solution. In order to clarify the effects of sintering temperature on the formation of dense perovskite membranes, all the hollow fibre precursor samples were prepared from the same starting solution with the composition of 66.67 wt% BCTb powder, 6.67 wt% PESf and 26.67 wt% NMP under similar spinning conditions. Fig. 1 demonstrates the microstructures of the BCTb hollow fibre precursor and the sintered hollow fibre membranes at different temperatures. As can be seen, the hollow fibre precursor possesses an asymmetric structure consisting of a relatively dense layer and a porous structure with a large number of macro voids evidenced by observation in Fig. 1-A1. It is a very typical structure of the membranes prepared by the phase inversion method when water is used as the external and the internal coagulants.[25] Fig. 1-A2 and A3 displays the outer and inner surfaces of the hollow fibre precursor, respectively. It can be recognized that the small BCTb particles were well dispersed and connected to each other by the polymer binder. Furthermore, the outer surface was much smoother than the inner surface. This may be attributed to the fact that the amount of the external coagulant for the solvent–nonsolvent exchange was much more than the internal coagulant, hence the precipitation rate occurring on the outside surface was much faster than that on the inner surface.[26] By sintering at an elevated temperature, i.e., 1250 °C, the polymer binder has been burnt out, forming a fairly porous structure in the hollow fibre, as observed in Fig. 1-B. As the sintering temperature was increased to 1300 or 1350 °C, further particle coalescence and bonding took place leading to shrinkage of the porous structure (Fig. 1-C and D). When the sintering temperature reached 1400 °C, the pores on the outer surface of the hollow fibre have almost disappeared, as can be seen in Fig. 1-E2. This implies that the fully densified layer near the outside surface would be achieved although the inner surface still maintains its porous structure. Such structural difference between the two surface layers after sintering was caused by the different local particle loading densities which existed in the precursor. Certainly, if sintered at sufficiently higher temperatures, the membrane layers near both surfaces will be completely

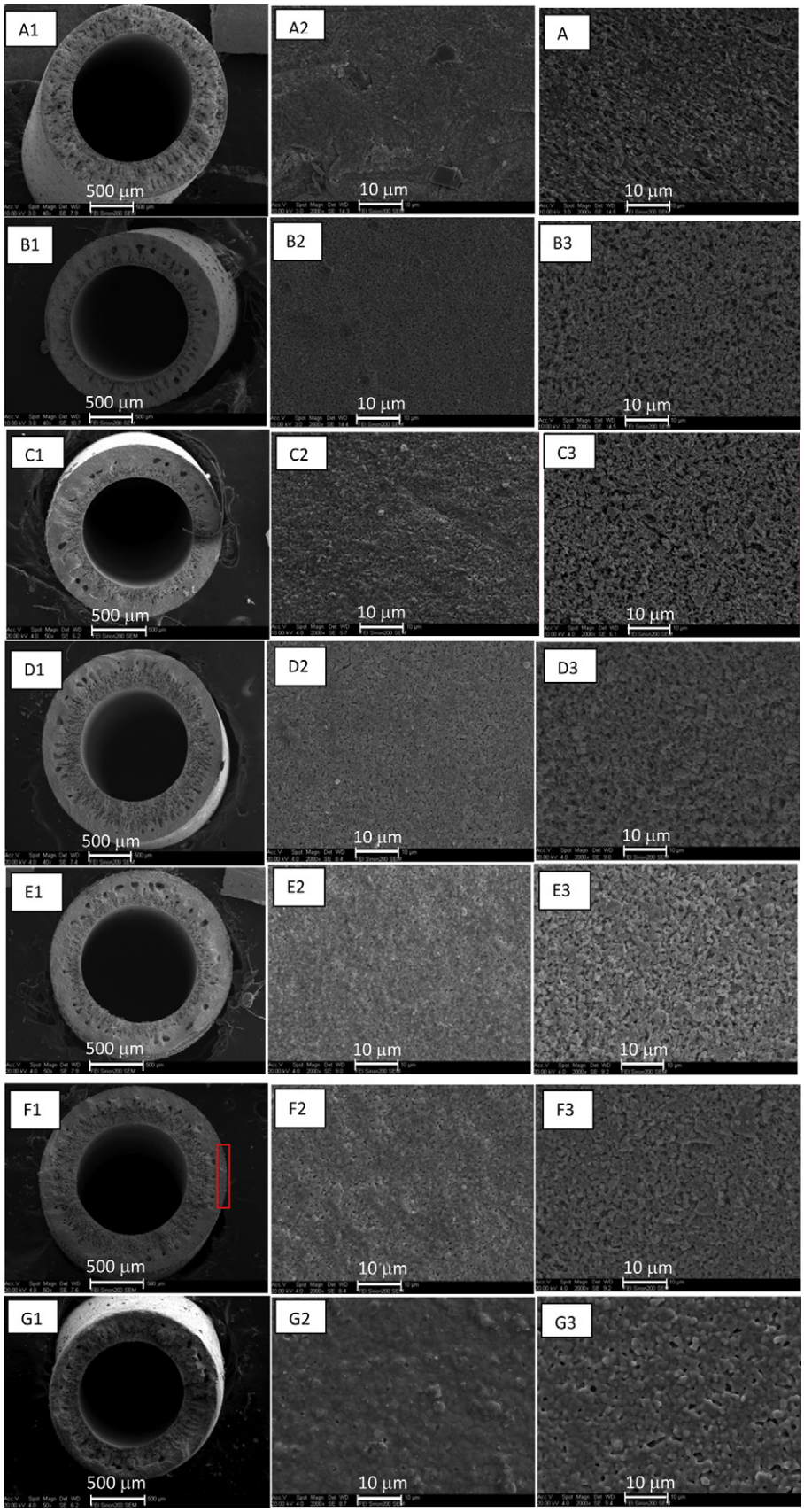

Fig. 1. SEM images of the BCTb hollow fibres (A) precursor and the membranes sintered at: (B) 1250 °C; (C) 1300 °C; (D) 1350 °C; (E) 1400 °C; (F) 1450 °C and (G) 1500 °C (1: cross-section; 2:outside surface; 3: inside surface). (For interpretation of the references to colour in this figure legend, the reader is referred to the web version of this article.)

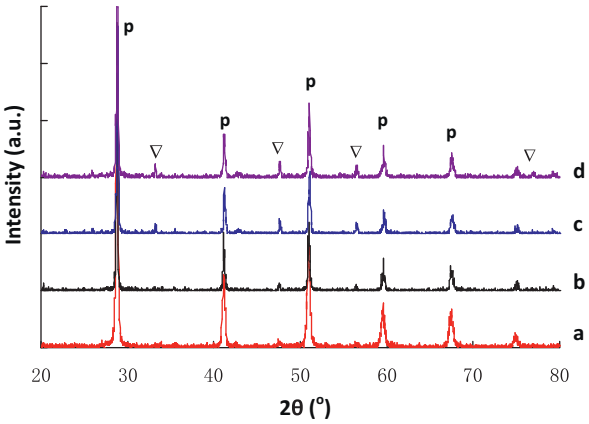

Fig. 2. XRD patterns of the BCTb hollow fibre membranes sintered at: (a) 1200 °C; (b) 1300 °C; (c) 1400 °C; (d) 1500 °C (p: perovskite; ∇: CeO_2 phase).

densified. The existence of the continuous densified layer after sintering at 1400 °C was confirmed by the gas permeation test with gas tightness at pressures up to 7 bars at room temperature. Further increases in the sintering temperature would promote grain growth by deep fusion and BCTb particle bonding. For example, after sintering at 1500 °C for 5 h, the grain size of the BCTb ceramic has increased up to 6 μm in contrast to the 0.1 μm of the staring particles, as is seen from Fig. 1-G3. Nevertheless, the macro voids were still preserved within the hollow fibres. This suggests that the general structure of the ceramic hollow fibres was mainly formed during the spinning process and could not be changed by the high temperature sintering. It should be mentioned that the densification of ceramic membranes into gas-tight structure is actually dependent not only on the sintering temperature but also on the particle loading density in the fibre precursors. In fact, we also have obtained the gas-tight hollow fibre membranes at a lower sintering temperature, i.e., 1350 °C when using a starting solution with higher powder content to spin the hollow fibre precursors.

Fig. 2 shows the XRD patterns of the BCTb hollow fibre membranes with different sintering temperatures. As can be seen, the original orthorhombic perovskite phase has been preserved well in the sintered hollow fibres. However, several impure diffraction peaks also occurred at (2θ) 33.26°, 47.7°, 56.6°, 75.1° and 77.2°, respectively when the sintering temperature was higher than 1300 °C. The intensity of these extra peaks would become stronger as the sintering temperature increased. Analysis using the MDI Jade 5.0 software indicates these impure peaks belong to the CeO_2 phase (PDF reference code 34-0394). This phenomenon can be explained by the phase separation at higher temperatures near the melting point (1480 °C) of $BaCeO_3$ at which $BaCeO_3$ will be separated into solid phase CeO_2 and a liquid phase rich of BaO.[27] At such a high temperature, the liquid BaO is easily evaporated, which not only alters the initially designed material composition but also deteriorates the mechanical strength. Looking back to the SEM image of the cross sectional area in Fig. 1-G1, the overall integral structure of the hollow fibre was also altered by such phase separating behaviour.

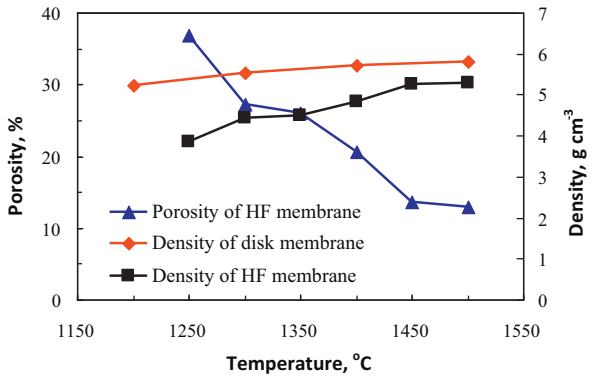

Fig. 3. Apparent density and porosity of the BCTb hollow fibres sintered at different temperatures.

Fig. 3 shows the apparent density and porosity of the BCTb hollow fibre membranes as a function of sintering temperature and the apparent density of the disk membrane is also presented for comparison purposes. As is expected, the apparent density of the BCTb disk membrane slightly increased with the sintering temperature because the densification of ceramics could be promoted by a higher temperature. The theoretical density of the BCTb perovskite was calculated from the XRD lattice constants to be 6.314 g cm^{-3}. Therefore, the relative density of the BCTb disk ranged from 87.1% to 96.5% as the sintering temperature increased from 1200 °C to 1500 °C. From the apparent density data, the porosity of the hollow fibre membranes could be calculated as also presented in Fig. 3. As can be seen, the porosity of the hollow fibres decreased dramatically from 36.8% at 1200 °C to 13.6% at 1450 °C but then decreased slightly to 12.9% as the sintering temperature was further increased to 1500 °C.

The sufficient mechanical strength of the ceramic hollow fibre membranes is an important prerequisite for them to be assembled inside membrane modules for practical applications. Fig. 4 shows the mechanical property of the BCTb hollow fibres in terms of three-point bending strength as a function of sintering temperature. As can be seen, the membrane sintered at temperatures lower than 1200 °C was very weak with a bending strength value about 30.3 MPa. However, when the sintering temperature is higher than 1400 °C, the mechanical strength was increased to 130.4 MPa, which is sufficiently robust for the fabrication

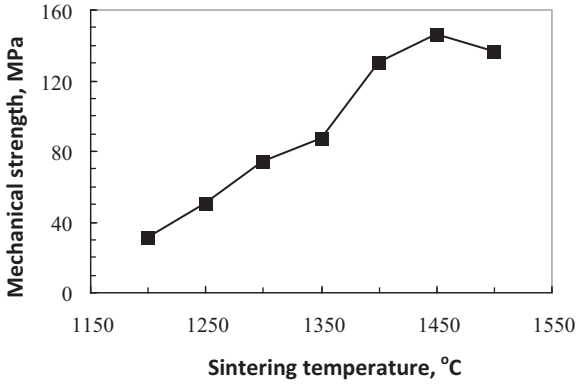

Fig. 4. Mechanical strength of the BCTb hollow fibres as a function of sintering temperature.

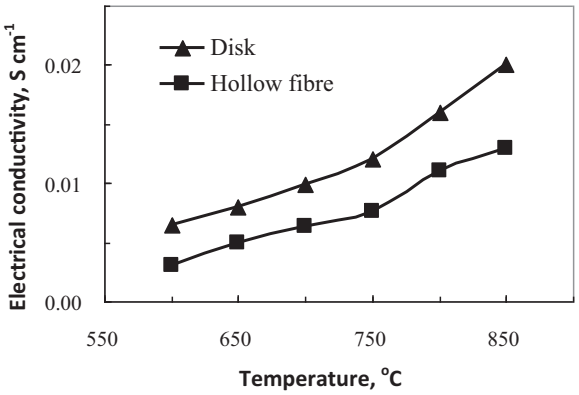

Fig. 5. The electrical conductivity of the BCTb disk and the hollow fibre as a function of temperature.

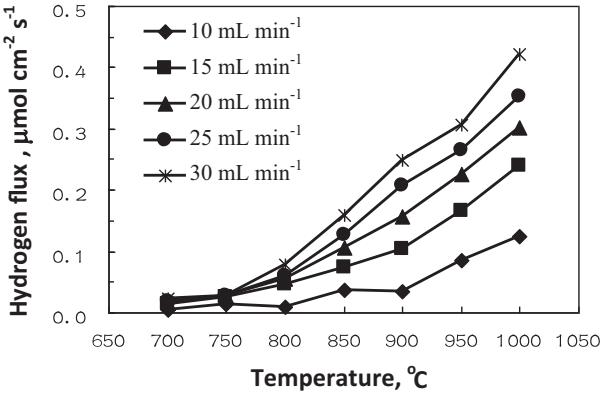

Fig. 6. Hydrogen permeation fluxes through the 1400 °C-sintered BCTb hollow fibre membrane with different N_2 sweep flow rates (50% H_2–He feed flow rate = 40 mL min^{-1}).

of fibre modules. Such improvement in mechanical strength is achieved by the increased densification at higher sintering temperatures. Fig. 4 also shows that there exists an optimum value of the sintering temperature (1450 °C) at which the sintered hollow fibres have a maximum bending strength of 146 MPa. After this optimum temperature (1450 °C), the mechanical strength of the membrane starts to drop, for example, with a lower value of 137 Mpa at 1500 °C. This can be explained by the phase separation of the membrane materials at high temperatures near the melting point of 1480 °C of $BaCeO_3$ as observed in the XRD patterns in Fig. 2d and from the SEM image from the cross sectional area in Fig. 1-G1.

The electrical conduction property of ceramic membranes is another important parameter for gas permeation since the permeation is based on the ionic transportation in the membrane bulk. Fig. 5 shows the temperature dependence of conductivity of the sintered BCTb hollow fibre membranes at 1400 °C for 5 h. For comparison purpose, the conductivity data of the BCTb disk sintered under similar conditions (1450 °C for 10 h) were also plotted in the figure. As can be seen, both the BCTb hollow fibre and the disk exhibited enhanced electrical conductivity as the measurement temperature increased. However, the conductivity of the BCTb disk was constantly higher than that of the hollow fibre in the entire temperature measurement range. For example, the BCTb disk exhibited the maximum electrical conductivity of 0.02 S cm^{-1} at 850 °C, which is almost twice the maximum conductivity of the BCTb hollow fibres (~0.013 S cm^{-1}) at the same temperature. Such distinction might result from the difference in the microstructures of the pressed disk and the porous hollow fibres derived by phase inversion. As described above, there are considerable macro voids inside the hollow fibres. Such macro voids could impede the ionic transportation and thus suppress the proton conduction of the hollow fibre membranes.

3.2. Hydrogen permeation

Hydrogen permeation tests were conducted on the BCTb hollow fibre membranes sintered at 1400 °C because these hollow fibres had high mechanical strength, few impurity phases and more importantly, were completely gas-tight. Fig. 6 shows the experimental results with the hydrogen permeation fluxes plotted against measurement temperature where the feed flow rate of the H_2–He mixture was fixed at 40 mL min^{-1} and the nitrogen sweeping rate ranged from 10 to 30 mL min^{-1}. It can be observed that the maximum H_2 permeation flux through the BCTb hollow fibre membrane could reach up to 0.422 μmol cm^{-2} s^{-1} (or 0.57 mL (STP) cm^{-2} min^{-1}) at 1000 °C with the N_2 sweep flow rate of 30 mL min^{-1}. This flux is almost one order of magnitude higher than the literature values reported for the similar proton conducting oxide membranes. For example, the hydrogen permeation fluxes through the $BaCe_{0.95}Nd_{0.05}O_{3-\delta}$[6] and $BaCe_{0.9}Mn_{0.1}O_{3-\delta}$[28] dense ceramic membranes were only 0.013 μmol cm^{-2} s^{-1} at 925 °C with membrane thickness of 0.7 mm and 0.011 μmol cm^{-2} s^{-1} at 900 °C with a membrane thickness of 1.06 mm, respectively. Such a drastic increase in hydrogen permeation flux can be attributed to the improved ionic conductivity of the BCTb membrane, the reduced membrane thickness with example shown in Fig. 1-F1 (marked with red rectangle shape) of less than 100 μm and inner porous surface to facilitate the surface reactions. Generally, the hydrogen flux through a mixed proton–electron conducting membrane can be expressed by the Wagner equation, which is derived on the basis of bulk diffusion as the rate limiting step:

$$J_{H_2} = \frac{RT}{4F^2L}\int_{p'_{H_2}}^{p''_{H_2}} \frac{\sigma_{OH^\bullet}(\sigma_{h^\bullet} + \sigma_{e'})}{\sigma_t} d\ln p_{H_2} \quad (4)$$

where σ_i is the conductivity of species i; L is the thickness of the membrane and the subscripts $OH^\bullet$, $h^\bullet$ and e' stand for proton, electron hole and electron, respectively. According to Eq. (4), the hydrogen flux is inversely proportional to the membrane thickness. In the phase-inversion induced hollow fibre membranes, the effective membrane thickness for hydrogen permeation may be actually much lower than the apparent wall thickness of the fibre due to the asymmetric structure. Of course, the clarification of the detailed reason or mechanism for such improvement still needs much more work, i.e., to compare the performance of a series of BCTb hollow fibres with different thickness and surface morphologies, which will be reported in our future work.

In addition, Fig. 6 also demonstrates the general trend of gas permeation through the perovskite membranes. As is expected, the hydrogen flux increased with increasing temperature since both the surface reaction kinetics and the bulk ionic diffusion could be promoted by the use of higher temperatures. For example, the hydrogen flux rose from 0.022 to 0.422 $\mu mol\,cm^{-2}\,s^{-1}$ as the temperature was increased from 700 °C to 1000 °C when the nitrogen sweeping rate was kept 30 mL min^{-1}. On the other hand, the hydrogen flux increased with increasing the nitrogen sweep flow rate at a given permeation temperature, which may be directly attributed to the lowering of hydrogen partial pressure at the permeate side. For example, increasing the nitrogen flow rate from 10 to 30 mL min^{-1} boosted the hydrogen flux at 900 °C from 0.035 to 0.25 $\mu mol\,cm^{-2}\,s^{-1}$. These trends were also repetitively observed in the operation of the mixed conducting ceramic membrane for oxygen production or separations.[23,24]

4. Conclusions

Gas-tight $BaCe_{0.95}Tb_{0.05}O_{3-\alpha}$ (BCTb) perovskite hollow fibre membranes have been fabricated by the combined phase inversion and sintering technique. The starting membrane material, the BCTb powder precursor synthesized by the sol–gel method has to be calcined at 1000 °C to form the perovskite structure. The sintering temperature has significant effect on the properties of the resultant BCTb hollow fibre membranes. In order to obtain gas-tight and robust hollow fibre membranes, the sintering temperature should be controlled between 1350 and 1450 °C. The hydrogen permeation fluxes through the BCTb hollow fibre membranes increase with temperature and the maximum fluxes can reach up to 0.422 $\mu mol\,cm^{-2}\,s^{-1}$ at 1000 °C when the flow rates of the H_2–He mixture feed and the nitrogen sweeping were 40 mL min^{-1} and 30 mL min^{-1}, respectively.

Acknowledgements

The authors gratefully acknowledge research funding from the Natural Science Foundation of China (Nos. 20976098 and 21176187), Natural Science Foundation of Shandong Prov. (No. Y2008B07) and Tianjin Research Program of Application Foundation and Advanced Technology (11JCZDJC23400). Dr. Shaomin Liu from Curtin University and Dr. Kayleen Campbell from the University of Queensland gave much help to improve the English writing of the this paper.

References

1. Iwahara H. Technological challenges in the application of proton conducting ceramics. *Solid State Ionics* 1995;**77**:289–98.
2. Iwahara H. Hydrogen pumps using proton-conducting ceramics and their applications. *Solid State Ionics* 1999;**125**:271–8.
3. Norby T, Larring Y. Mixed hydrogen ion–electronic conductors for hydrogen permeable membranes. *Solid State Ionics* 2000;**136–137**:139–48.
4. Marnellos G, Zisekas S, Stoukides M. Synthesis of ammonia at atmospheric pressure with the use of solid state proton conductors. *J Catal* 2000;**193**:80–7.
5. Liu S, Tan X, Li K, Hughes R. Methane coupling using membrane reactors. *Catal Rev* 2001;**43**:147–98.
6. Cai M, Liu S, Efimov K, Caro J, Feldhoff A, Wang H. Preparation and hydrogen permeation of $BaCe_{0.95}Nd_{0.05}O_{3-\delta}$ membranes. *J Membr Sci* 2009;**343**:90–6.
7. Iwahara H, Asakura Y, Katahira K, Tanaka M. Prospect of hydrogen technology using proton-conducting ceramics. *Solid State Ionics* 2004;**168**:299–310.
8. Song SJ, Moon JH, Ryu HW, Lee TH, Dorris SE, Balachandran U. Non-galvanic hydrogen production by water splitting using cermet membranes. *J Ceram Process Res* 2008;**9**:123–5.
9. Qi X, Lin YS. Electrical conducting properties of proton-conducting terbiumdoped strontium cerate membrane. *Solid State Ionics* 1999;**120**: 85–93.
10. Qi X, Lin YS. Electrical conduction and hydrogen permeation through mixed proton–electron conducting strontium cerate membranes. *Solid State Ionics* 2000; **130**:149–56.
11. Wei X, Kniep J, Lin YS. Hydrogen permeation through terbium doped strontium cerate membranes enabled by presence of reducing gas in the downstream. *J Membr Sci* 2009;**345**:201–6.
12. Cheng S, Gupta VK, Lin JYS. Synthesis and hydrogen permeation properties of asymmetric proton-conducting ceramic membranes. *Solid State Ionics* 2005;**176**:2653–62.
13. Zhana S, Zhu X, Ji B, Wang W, Zhang X, Wang J, et al. Preparation and hydrogen permeation of $SrCe_{0.95}Y_{0.05}O_{3-\delta}$ asymmetrical membranes. *J Membr Sci* 2009;**340**:241–8.
14. Hamakawa S, Li L, Li A, Iglesia E. Synthesis and hydrogen permeation properties of membranes based on dense $SrCe_{0.95}Yb_{0.05}O_{3-\alpha}$ thin films. *Solid State Ionics* 2002;**148**:71–81.
15. Zhan S, Zhu X, Ji B, Wang W, Zhang X, Wang J, et al. Preparation and hydrogen permeation of $SrCe_{0.95}Y_{0.05}O_{3-\delta}$ asymmetrical membranes. *J Membr Sci* 2009;**340**:241–8.
16. Luyten J, Buekenhoudt A, Adriansens W, Cooymans J, Weyten H, Servaes F. Preparation of $LaSrCoFeO_{3-x}$ membranes. *Solid State Ionics* 2000;**135**:637.
17. Liu S, Tan X, Li K, Hughes R. Preparation and characterisation of $SrCe_{0.95}Yb_{0.05}O_{2.975}$ hollow fibre membranes. *J Membr Sci* 2001;**193**:249–60.
18. Tan X, Liu Y, Li K. Preparation of LSCF ceramic hollow fiber membranes for oxygen production by a phase-inversion/sintering technique. *Ind Eng Chem Res* 2005;**44**:61.
19. Schiestel T, Kilgus M, Peter S, Caspary KJ, Wang H, Caro J. Hollow fibre perovskite membranes for oxygen separation. *J Membr Sci* 2005;**258**:1.
20. Lui S, Gavalas GR. Oxygen selective ceramic hollow fibre membranes. *J Membr Sci* 2005;**246**:103.
21. Liu Y, Li K. Preparation of $SrCe_{0.95}Yb_{0.05}O_{3-\alpha}$ hollow fibre membranes: study on sintering processes. *J Membr Sci* 2005;**259**:47–54.
22. Meng X, Yang N, Song J, Tan X, Ma Z, Li K. Synthesis and characterization of terbium doped barium cerates as a proton conducting SOFC electrolyte. *Int J Hydrogen Energy* 2011;**36**:13067–72.
23. Tan X, Liu Y, Li K. Mixed conducting ceramic hollow fiber membranes for air separation. *AIChE J* 2005;**51**:1991–2000.
24. Meng B, Wang Z, Tan X, Liu S. $SrCo_{0.9}Sc_{0.1}O_{3-\delta}$ hollow fibre membranes for oxygen separation at intermediate temperatures. *J Eur Ceram Soc* 2009;**29**:2815–22.
25. Tan X, Liu N, Meng B, Liu S. Morphology control of perovskite hollow fibre membranes for oxygen separation using different bore fluids. *J Membr Sci* 2011;**378**:308–18.
26. Xu Z-L, Qusay FA. Polyethersulfone (PES) hollow fiber ultrafiltration membranes prepared by PES/non-solvent/NMP solution. *J Membr Sci* 2004;**239**:265–9.
27. Guha JP, Kolar D. Phase Equilibria in the system BaO–CeO_2. *J Mater Sci* 1971;**6**:1174–7.
28. Li GT, Xiong GX, Sheng SS, Yang WS. Hydrogen permeation properties of perovskite-type $BaCe_{0.9}Mn_{0.1}O_{3-\delta}$ dense ceramic membrane. *Chin Chem Lett* 2001;**12**:937.